An optical diffraction experiment for the advanced laboratory

S. A. Dodds
Physics Department, Rice University, Houston, Texas 77251

(Received 15 March 1989; accepted for publication 5 September 1989)

By treating scalar diffraction as a Fourier transform problem, it is possible to calculate the expected intensity patterns for arbitrary apertures using standard signal-processing software on a personal computer. This article presents a series of experiments on optical diffraction and spatial filtering phenomena, and quantitatively compares the results with calculations. Both the experimental and calculational methods are suitable for an advanced undergraduate laboratory.

I. INTRODUCTION

Diffraction phenomena hold a prominent place in the physics curriculum, as demonstrated by discussions in numerous textbooks and by frequent contributions to this Journal. The purpose of the present article is to show how modern computing tools and simple laboratory equipment can be applied to some of these diffraction experiments. Particular emphasis will be placed on measurements that lend themselves to straightforward analysis.

The basic idea is to treat scalar diffraction theory as a Fourier transform problem. This approach provides an obvious connection to the engineering curriculum and makes it easy to apply the very powerful signal-processing software available for personal computers. The numerical results for arbitrary apertures can be directly compared with measured intensities in both the Fraunhofer and Fresnel regimes, clearly demonstrating the success of the mathematical formalism. The same apparatus can be used to demonstrate the effect of removing various spatial frequency components from the images of slits and grids. More important, however, this approach provides a unified framework for diffraction calculations, which students otherwise tend to view as an assortment of obscure mathematical tricks.

Section II summarizes those elements of scalar diffraction theory needed to analyze the present experiments. This is followed by a description of several experiments utilizing one-dimensional apertures and their analysis with commercial signal-processing software. The article concludes with some suggestions for related projects that could be undertaken with the same apparatus.

II. THEORETICAL BACKGROUND

Within scalar diffraction theory both the Fresnel and Fraunhofer patterns produced by a planar aperture can be expressed as the Fourier transform of a source function. The form of the source function is easily specified in terms of the aperture transmission function and the incident illumination, allowing a complete numerical calculation of the resulting diffraction pattern. The same formalism is used to describe the effects of a thin lens as used in the spatial filtering experiments. The treatment generally follows Goodman's classic text,[1] which should be consulted for a more complete explanation. Similar discussions of some of the same subjects can be found in other optics texts and in earlier articles.[2]

A. Basic formalism

We start with the scalar wave equation

$$(\nabla^2 + k^2)\underline{E} = 0, \tag{1}$$

where $\underline{E}$ stands for the complex amplitude of one component of the optical field. The wavenumber k is defined by $k = 2\pi/\lambda$. This equation is to be solved for the geometry shown in Fig. 1, which depicts a planar aperture (the object) in an opaque screen illuminated from the left and an image plane at a distance z_i. We assume that the aperture can be represented as a collection of sources $\underline{E}_0(x_0, y_0)$ so that the field at each point in the image plane is the superposition of the fields due to those sources. For plane-wave illumination, as used here, $\underline{E}_0$ is simply the product of the incident amplitude A and a complex transmission function

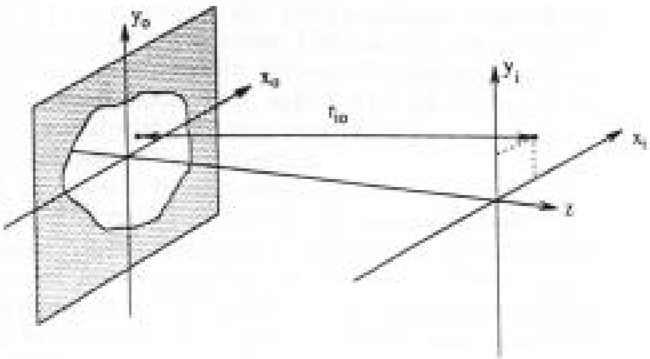

Fig. 1. Sketch of object- and image-plane coordinates showing the distance r_{io} between typical image and object points.

$T_0(x_0,y_0)$ that describes the phase shift and attenuation produced by the aperture.

Solutions to Eq. (1) are customarily sought in two regimes. The Fresnel approximation applies to the region of the image plane near the optic axis when z_i is much greater than the lateral extent of the aperture. In that case the solution can be expressed as a Fourier transform:

$$\underline{E}_i = [\exp(ikz_i)/i\lambda z_i]\exp[(ik/2z_i)(x_i^2+y_i^2)] \times \mathscr{F}_{z_i}\{\underline{E}_0 \exp[(ik/2z_i)(x_0^2+y_0^2)]\}. \quad (2)$$

The transform $\mathscr{F}_z(x,y)$ of a function $G(x_0,y_0)$ is defined by

$$\mathscr{F}_z\{G\} = \int\int G(x_0,y_0) \times \exp[-(ik/z)(x_0x+y_0y)]dx_0\,dy_0. \quad (3)$$

Note that this equation allows the student to calculate explicitly the Fresnel diffraction pattern for any aperture and illumination conditions.

If we move farther away from the aperture, so that

$$z_i \gg k(x_0^2+y_0^2)_{\max}, \quad (4)$$

the quadratic phase factor in Eq. (2) is approximately unity over the entire aperture. In this infinite-distance or Fraunhofer regime, the diffraction pattern is given by

$$\underline{E}_i = [\exp(ikz_i)/i\lambda z_i] \times \exp[(ik/2z_i)(x_i^2+y_i^2)]\mathscr{F}_{z_i}\{\underline{E}_0\}, \quad (5)$$

which is simply the Fourier transform of the aperture illumination within a phase factor. Since the optical intensity is proportional to $|\underline{E}|^2$, the phase is usually irrelevant.

B. Thin lenses and spatial filtering

With coherent illumination thin lenses can be used as spatial Fourier transformers, as well as for producing magnified images. To see how this occurs, consider a typical arrangement of point source, object transparency, and positive lens as shown in Fig. 2. The wave front from the source is successively modified by the transparency and the positive lens when [illegible]. We wish to large, thin lens and making the paraxial approximation,

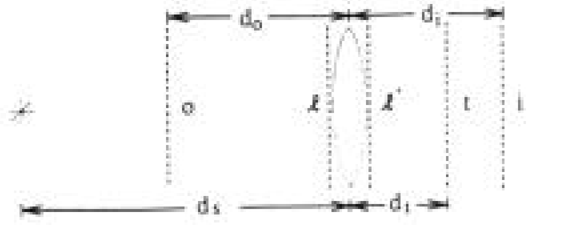

Fig. 2. Object, lens, transform, and image planes for a thin lens. A point source is located on the axis a distance d_s from the lens. The lens forms the Fourier transform of T_0 at plane t and a geometric image at plane i.

Goodman shows[1] that the disturbance at d_i is given by

$$\underline{E}_i = \frac{1}{M}\exp\left[\frac{ik}{2d_i}\left(1+\frac{1}{M}\right)(x_i^2+y_i^2)\right]\underline{E}_0\left(-\frac{x_i}{M},-\frac{y_i}{M}\right). \quad (6)$$

where $M = d_i/d_0$ is the geometric magnification. Except for a phase shift, $\underline{E}_i$ is a scaled copy of $\underline{E}_0$ and, for plane-wave illumination, of T_0. This result is obviously consistent with the usual geometrical optics condition for imaging.

Next, consider the transform plane, defined as the plane conjugate to the source: $(1/d_t) = (1/d_s) + 1/f$. For plane-wave illumination $d_s \to \infty$, $d_t = f$, and $\underline{E}_t$ takes the simple form

$$\underline{E}_t = (iA'/\lambda f) \times \exp[-(ik/2f^2)(d_0-f)(x_t^2+y_t^2)]\mathscr{F}_f\{T_0\}. \quad (7)$$

The image in the transform plane is evidently the spatial Fourier transform of the aperture transmission function. Equivalently, the transform plane displays the spatial frequency spectrum of the object.

A barrier (filter) placed in the transform plane can be used to modify the spatial frequency components making up the final image. The filter modifies the disturbance given by Eq. (7) according to $\underline{E}_t' = T_t(x_t,y_t)\underline{E}_t$. The modified wave then propagates to the final image plane at d_i. Some of the quadratic phase factors cancel, leaving

$$\underline{E}_i = (A'/\lambda^2 fz)\exp[ikz + ik(x_i^2+y_i^2)/2z] \times \int\int T_t\mathscr{F}_f\{T_0\} \times \exp[-(ik/z)(x_tx_i+y_ty_i)]dx_t\,dy_t, \quad (8)$$

where $z = d_i - f$. When $T_t = 1$, it follows immediately that $\underline{E}_i$ is the geometric image, consistent with Eq. (6).

III. EXPERIMENTS

A. Equipment and software

The experiments are readily done on a 2-m optical bench, although shorter benches could be used with appropriate choices of components. Various metal slits, mounted on a screw-driven transverse slide, were used as apertures. All the slits were long enough to be considered one-dimensional. The lens carriers should have provisions for trans- one end of the bench. The input is masked with a slit, typi-

cally 0.14 or 0.24 mm wide. The photometer output drives the y axis of an x-y recorder. The x axis of the recorder is driven by a potentiometer connected to the drive screw of the transverse slide. With appropriate adjustment of the recorder scales, this arrangement yields very reproducible plots of intensity versus position.

A low-power helium–neon laser is used as the light source. The results presented here were obtained with a nominal 5-mW laser, but a 1-mW unit has also been used with some loss of signal to noise. The beam must be aligned with the bench, either by deflecting the beam or moving the laser body. Once this is done, the laser beam is taken to define the optic axis, and the other components can be centered on it. Addition of a student-grade spatial filter does not noticeably affect the data, and so the beam is used unfiltered.

Simulated diffraction patterns are generated with a menu-driven commercial system[4] running on an IBM PC/XT with math coprocessor (required by the software). The input object is represented by a one-dimensional 1024-element array in which "ones" denote transparent regions. The array is multiplied by a complex phase factor if needed and Fourier transformed to obtain the diffraction pattern. Spatial filtering is done by transforming the input array, multiplying by a filter function represented as a binary array, and then transforming again. An entire simulation cycle of paramter setting, calculation, and intensity plotting can be done in well under 1 min.

Some precautions are necessary in doing these calculations. The size of the input pattern must be chosen to give adequate resolution in both the input and the transform. Further, the finite transform begins to deviate noticeably from the exact transform at about one-half of the Nyquist frequency (one-quarter the size of the transform array). The input pattern must be wide enough that little power falls in this region. Patterns that are too wide lead to rapid oscillation of the phase factor $\exp(ikx^2/z)$ and loss of accuracy in Fresnel calculations. Input widths of 5%–50% of the array width seem to be a reasonable compromise for the software and array sizes used here.

B. Fraunhofer diffraction

The optical bench is long enough to reach the Fraunhofer regime for small apertures.[5] The desired object is simply placed in the laser beam and the distance z, adjusted, subject to Eq. (4), to obtain a pattern of convenient size. The theoretical intensities are found by computing the power spectrum of the input array. Since Fraunhofer patterns are geometrically similar, no adjustment of parameters is needed to compare with the measurements. Typical results are shown in Fig. 3 for a simple multislit object. The agreement is obviously good, and much more detail can be observed by expanding the vertical scale in both plots.

A more stringent test of the Fraunhofer diffraction calculation is shown in Fig. 4. The object is a single slit, for which the diffracted intensity is known to be proportional to $(\sin x/x)^2$. The points are the measured intensities of the first 18 subsidiary maxima, normalized to the intensity of the $x=0$ peak. The finite size (about 5-mm diam) of the laser beam does not influence the relative intensities. Measurements were made with both 0.14- and 0.24-mm photometer apertures to verify that the slit was narrow enough to resolve the peaks. It was also necessary to calibrate the photometer using a set of neutral density filters, since the instrument used is significantly nonlinear over such a wide range of intensity.

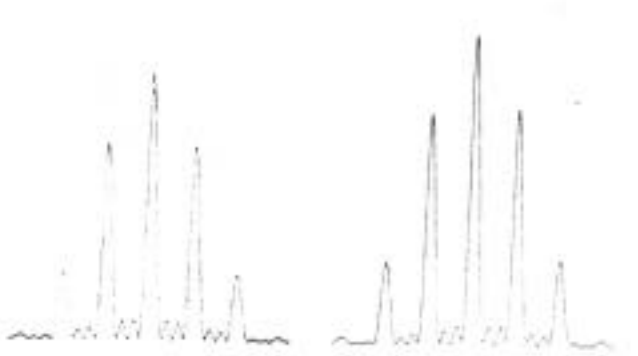

Fig. 3. Fraunhofer diffraction pattern from four slits, 0.04 mm wide on 0.125-mm centers. Left: intensity versus position calculated from Eq. (5) using the given ratio of slit width to separation. Right: measured intensity versus position at a plane 60 cm from the slits. The pattern was scanned with a 0.14-mm aperture over a range of 2.8 cm.

The agreement between the data, the finite Fourier transform, and the exact calculation is acceptable over about three orders in intensity. Beyond the tenth peak the measured total intensities are larger than expected from the exact calculation due to the presence of a diffuse background. If the background is subtracted, the peaks are in fact smaller than calculated by about a factor of 2. The problem has been noted before,[6] but not satisfactorily explained. (The phenomenon does not arise in the photometer since the loss of fringe contrast is evident by eye. It is

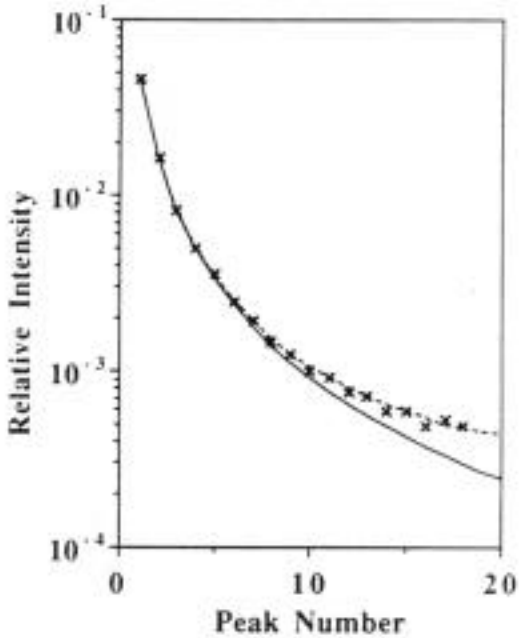

finite Fourier transform of a unit pulse 50 channels wide, centered in a 1024-channel array.

also insensitive to the nature of the slits.) Coincidentally, the limitations of the finite Fourier transform, as noted above, also affect the intensities in this range.

The loss of high spatial frequencies is not readily observable in most other measurements since the total power at those frequencies is quite small. Some deviations are, however, seen in spatial filtering experiments, particularly when the strong central peak is suppressed. For those measurements it is better to remove deliberately the higher frequencies when making comparisons with calculated patterns.

C. Fresnel diffraction

The Fresnel patterns are, of necessity, about the same size as the diffracting object. It is therefore convenient to use a lens to project a 10–50× magnified image onto the photometer. This is done by placing the object and lens on the bench, and adjusting the object position to obtain a sharp image at the photometer. By sliding the object farther away from the lens, one can then image planes a known distance beyond the object.

The initial focus is easier to find if white light is used, or if a diffuser is temporarily placed in the laser beam ahead of the object. Otherwise, there is a tendency to focus for visually sharp edges, resulting in large intensity peaks at the edge of the image. It will usually be necessary to adjust the lateral position of the object a few tenths of a millimeter to obtain a symmetric pattern. This is readily accomplished when the object position is set to give a simple diffraction pattern. It is somewhat easier to symmetrize the diffraction pattern if the laser beam is expanded, but the loss of intensity may be unacceptable.

The computational scheme follows directly from Eq. (2). The input array is multiplied by $\exp\left[(i\gamma)(x_0^2+y_0^2)\right]$, where γ is a real scale factor determined by the resolution of the array. The power spectrum of the product is then computed and plotted to an appropriate scale for comparison with the experiment. Variation in the object distance is simulated by scaling the extent of the object in the input array, with broader objects corresponding to closer obser-

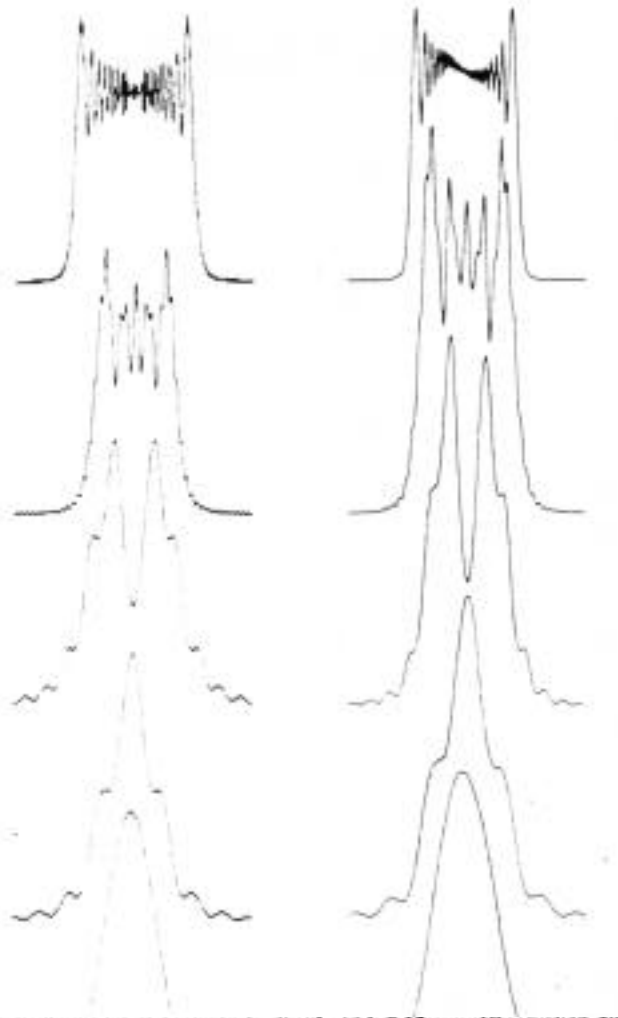

diffraction patterns for a single slit of width 0.37 mm. Observation distance increases top to bottom from 0.2 to 14.0 cm.

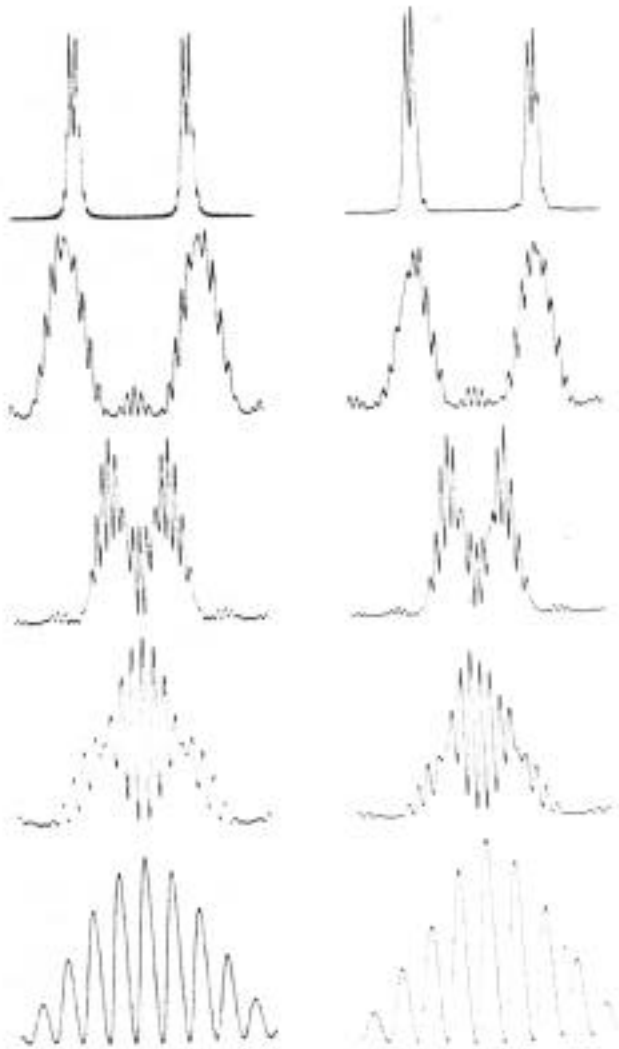

Fig. 6. Comparison of calculated (left) and measured (right) Fresnel [illegible] was used to obtain a magnification of [illegible] images.

vation planes. As noted above, some care is needed to insure numerical accuracy.

Several single-slit patterns are displayed in Fig. 5. The agreement with the calculated patterns is generally satisfactory. Within the accuracy of the equipment, these results also compare favorably with a much more detailed study done with large-scale apparatus.[7] Note, however, that the experimental curves are slightly asymmetric, presumably due to inaccurate centering of the slit and nonuniformity in the input beam. The very fine detail present in some of the numerical results is lost due to the finite width of the photometer aperture, here about 3% of the image width.

Examples of more complicated Fresnel patterns produced by a double slit are shown in Fig. 6. One sees that at short distances there are two separate single-slit Fresnel patterns. As the distance increases, there is progressive overlap and modification of the separate patterns until something resembling a two-slit Fraunhofer pattern emerges. Lock has recently noted the same phenomenon in his calculations.[8] (The magnification needed to display the near-slit pattern makes it impossible to reach the true Fraunhofer regime.)

D. Spatial filtering

Spatial filtering was done with an expanded beam, achieved by collimating the input beam with a 10× microscope objective and 5-cm lens. The focal length of the lens used as the Fourier transformer was chosen to give a reasonable compromise between the size of the transform image (proportional to f) and of the geometric image (inversely proportional to f for fixed bench length much greater than f). Using $f = 17$ cm on the 2-m bench gave a final image magnification of about 8×, making an auxiliary lens unnecessary for the objects used. This greatly simplifies the focus adjustment.

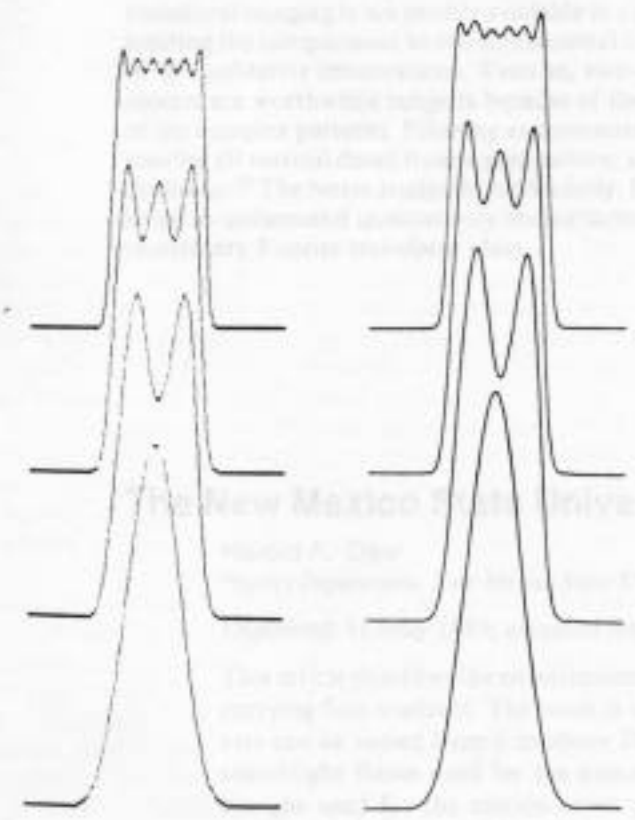

Fig. 7. Filtered image of a 0.16-mm slit (right) compared with calculation [illegible] with a unit pulse corresponding to the photometer width of 0.14 mm, about 12% of the image width.

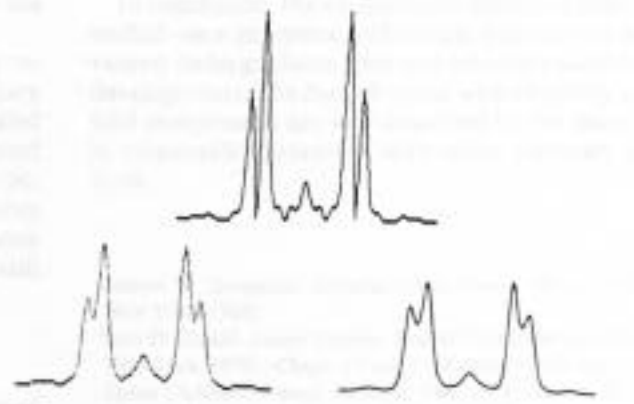

Fig. 8. Image of a 0.16-mm slit when the first five subsidiary peaks only are transmitted. The upper image is a simulation at full resolution. The lower images show the effect of the finite photometer slit width on the calculated (left) and measured (right) intensities.

Filtering was done at the transform plane by inserting paper cards to block the unwanted Fourier components. A ground-glass screen and magnifier temporarily inserted just beyond the transform plane aids in adjusting the "filter." For the measurements shown in Figs. 7 and 8, the filter cutoff points were placed at intensity minima in the transform plane. Other positions can be used, of course, but this choice makes it very easy to obtain corresponding experimental and simulated filter functions.

Patterns are calculated by Fourier transforming the input array as usual. The desired filter transmission function is represented by a simillar array with "ones" where the simulated filter is to pass light and "zeros" otherwise. The filter array is easily designed by referring to the power spectrum of the input array. From Eq. (8) the power spectrum of the product of the transform and the filter function is the desired output. After filtering, the simulated image can be convolved with a rectangular pulse representing the finite slit width of the photometer. In principle, this should be done with all the simulations, but the larger magnifications used in the other experiments make the blurring insignificant.

The filtered image of the slit displays a number of interesting phenomena, as first demonstrated by Duffieux *et al.*[6] in 1944. Figure 7 shows the effect of increases in the transmitted bandwidth obtained by including up to five subsidiary maxima of the transform. Addition of each additional subsidiary maximum adds another "wiggle" to the image, just as summation of successive Fourier series terms son for this is apparently the loss of high-frequency information discussed in Sec. III B. The only effect of the wide

vation planes. As noted above, some care is needed to insure numerical accuracy.

Several single-slit patterns are displayed in Fig. 5. The agreement with the calculated patterns is generally satisfactory. Within the accuracy of the equipment, these results also compare favorably with a much more detailed study done with large-scale apparatus.[7] Note, however, that the experimental curves are slightly asymmetric, presumably due to inaccurate centering of the slit and nonuniformity in the input beam. The very fine detail present in some of the numerical results is lost due to the finite width of the photometer aperture, here about 3% of the image width.

Examples of more complicated Fresnel patterns produced by a double slit are shown in Fig. 6. One sees that at short distances there are two separate single-slit Fresnel patterns. As the distance increases, there is progressive overlap and modification of the separate patterns until something resembling a two-slit Fraunhofer pattern emerges. Lock has recently noted the same phenomenon in his calculations.[8] (The magnification needed to display the near-slit pattern makes it impossible to reach the true Fraunhofer regime.)

D. Spatial filtering

Spatial filtering was done with an expanded beam, achieved by collimating the input beam with a 10× microscope objective and 5-cm lens. The focal length of the lens used as the Fourier transformer was chosen to give a reasonable compromise between the size of the transform image (proportional to f) and of the geometric image (inversely proportional to f for fixed bench length much greater than f). Using $f = 17$ cm on the 2-m bench gave a final image magnification of about 8×, making an auxiliary lens unnecessary for the objects used. This greatly simplifies the focus adjustment.

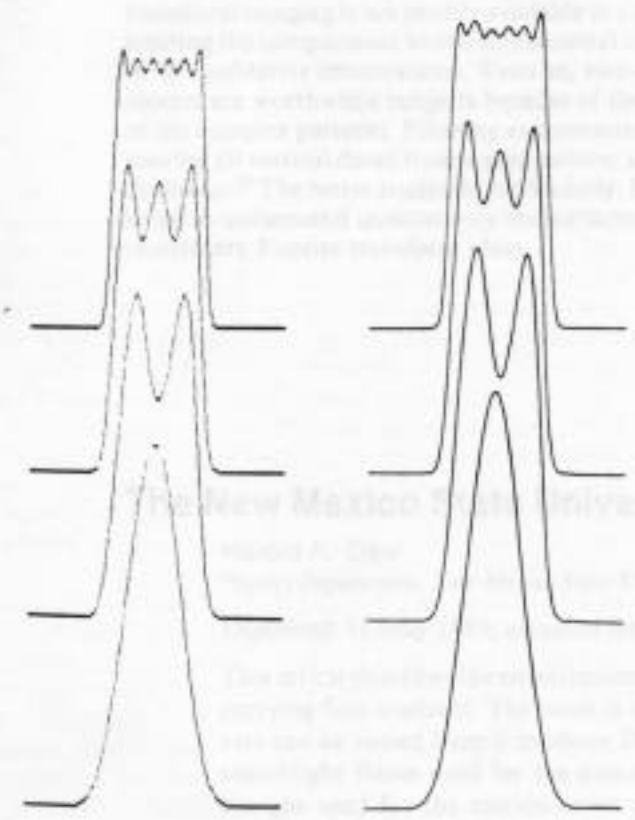

Fig. 7. Filtered image of a 0.16-mm slit (right) compared with calculation [illegible] with a unit pulse corresponding to the photometer width of 0.14 mm, about 12% of the image width.

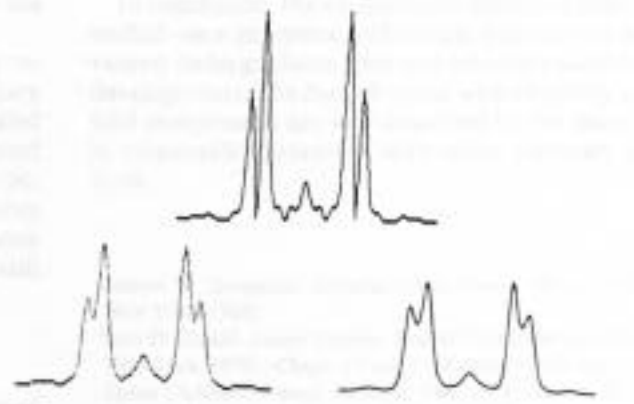

Fig. 8. Image of a 0.16-mm slit when the first five subsidiary peaks only are transmitted. The upper image is a simulation at full resolution. The lower images show the effect of the finite photometer slit width on the calculated (left) and measured (right) intensities.

Filtering was done at the transform plane by inserting paper cards to block the unwanted Fourier components. A ground-glass screen and magnifier temporarily inserted just beyond the transform plane aids in adjusting the "filter." For the measurements shown in Figs. 7 and 8, the filter cutoff points were placed at intensity minima in the transform plane. Other positions can be used, of course, but this choice makes it very easy to obtain corresponding experimental and simulated filter functions.

Patterns are calculated by Fourier transforming the input array as usual. The desired filter transmission function is represented by a simillar array with "ones" where the simulated filter is to pass light and "zeros" otherwise. The filter array is easily designed by referring to the power spectrum of the input array. From Eq. (8) the power spectrum of the product of the transform and the filter function is the desired output. After filtering, the simulated image can be convolved with a rectangular pulse representing the finite slit width of the photometer. In principle, this should be done with all the simulations, but the larger magnifications used in the other experiments make the blurring insignificant.

The filtered image of the slit displays a number of interesting phenomena, as first demonstrated by Duffieux *et al.*[6] in 1944. Figure 7 shows the effect of increases in the transmitted bandwidth obtained by including up to five subsidiary maxima of the transform. Addition of each additional subsidiary maximum adds another "wiggle" to the image, just as summation of successive Fourier series terms son for this is apparently the loss of high-frequency information discussed in Sec. III B. The only effect of the wide

photometer slit is to decrease slightly the amplitude of the variations in the image.

More dramatic patterns can be produced by totally removing the central maximum while passing five subsidiary maxima on either side, as shown in Fig. 8. The calculated pattern shows bright regions split by a dark line located precisely at the slit edge. Again, a similar phenomenon occurs if the fundamental is suppressed in the Fourier series description of a square wave. Smoothing by the photometer slit reduces the variation noticeably, but the effect can still be seen in both calculation and measurement.

IV. EXTENSIONS AND CONCLUSIONS

Diffraction patterns have been shown for a number of one-dimensional objects to illustrate the capabilities of the equipment. The same methods could be applied to arbitrarily complicated items such as gratings (amplitude or phase), nonperiodic arrays, gray-scale transparencies, and phase-shift objects. Filtering experiments could be designed to explore Abbe imaging theory, phase-contrast microscopy, optical noise reduction, and optical pattern matching.[2,9] It might also be desirable to use a data-acquisition board to read the position and intensity data for a quantitative comparison with the theory. That would, however, require careful normalization of the scales and extensive computation, a time-consuming prospect.

With sufficient computational power, or patience, the formalism can be used to simulate two-dimensional diffraction and filtering experiments.[9] Unfortunately, two-dimensional imaging is not readily available in a teaching lab, limiting the comparisons to one-dimensional cross sections or to qualitative observations. Even so, two-dimensional objects are worthwhile subjects because of the fascination of the complex patterns. Filtering experiments, such as removing all vertical detail from a grid pattern, are also more dramatic.[10] The better students, particularly, find it a challenge to understand qualitatively the patterns in terms of elementary Fourier transform ideas.

In conclusion, the experiments described here present a unified view of optical diffraction phenomena at the advanced undergraduate level and provide a basis for further developments. The data obtained with relatively simple optical components are well described by the theory and are in reasonable agreement with more elaborate investigations.

[1]Joseph W. Goodman, *Introduction to Fourier Optics* (McGraw-Hill, New York, 1968).

[2]Jack D. Gaskill, *Linear Systems, Fourier Transforms and Optics* (Wiley, New York, 1978), Chaps. 10 and 11; Eugene Hecht and Alfred Zajac, *Optics* (Addison-Wesley, Reading, MA, 1974), Chaps. 10, 11, and 14; James E. Harvey, "Fourier treatment of near-field scalar diffraction theory," Am. J. Phys. **47**, 974–980 (1979); C. W. Curtis and W. J. van Sciver, "Diffraction, transforms and spatial filtering," Am. J. Phys. **40**, 1684–1687 (1972); Judith C. Brown, "Fourier analysis and spatial filtering," Am. J. Phys. **39**, 797–801 (1971); Richard A. Phillips, "Spatial filtering experiments for undergraduate laboratories," Am. J. Phys. **37**, 536–540 (1969).

[3]"High Sensitivity Photometer," Model OS-8020.01, Pasco Scientific, 10101 Foothills Blvd., Roseville, CA 95678.

[4]"ASYSTANT +," Asyst Software Technologies, Inc., 100 Corporate Woods, Rochester, NY 14623.

[5]"Precision Electroformed Slits," Pasco Scientific. The largest patterns in this set require $z \geqslant 60$ cm.

[6]Michel Duffieux, Jean Tirouflet, Henri Guenoche, and Guy Lansraux, "Image d'une fente en eclairage coherent," Ann. Phys. (Paris) **19**, 355–395 (1944).

[7]Franklin S. Harris, Jr., Michael S. Tavenner, and Richard L. Mitchell, "Single-slit Fresnel diffraction patterns: Comparison of experimental and theoretical results," J. Opt. Soc. Am. **59**, 293–296 (1969).

[8]James A. Lock, "Numerical methods in optics: A course about learning physics through computing," Am. J. Phys. **55**, 1121–1125 (1987).

[9]T. A. Wiggins, "Hole gratings for optics experiments," Am. J. Phys. **53**, 227–229 (1985); D. S. Burch, "Fresnel diffraction by a circular aperture," Am. J. Phys. **53**, 255–260 (1985); Xiangxi Chen, Jacob Huang, and Eddie Loh, "Two-dimensional fast Fourier transform and pattern processing with IBM PC," Am. J. Phys. **56**, 747–749 (1988).

[10]See texts by Gaskill or Hecht and Zajac, Ref. 2, for photographs.